

# Organic & Biomolecular Chemistry

Accepted Manuscript



This is an *Accepted Manuscript*, which has been through the Royal Society of Chemistry peer review process and has been accepted for publication.

*Accepted Manuscripts* are published online shortly after acceptance, before technical editing, formatting and proof reading. Using this free service, authors can make their results available to the community, in citable form, before we publish the edited article. We will replace this *Accepted Manuscript* with the edited and formatted *Advance Article* as soon as it is available.

You can find more information about *Accepted Manuscripts* in the [Information for Authors](#).

Please note that technical editing may introduce minor changes to the text and/or graphics, which may alter content. The journal's standard [Terms & Conditions](#) and the [Ethical guidelines](#) still apply. In no event shall the Royal Society of Chemistry be held responsible for any errors or omissions in this *Accepted Manuscript* or any consequences arising from the use of any information it contains.

Cite this: DOI: 10.1039/c0xx00000x

www.rsc.org/xxxxxx

ARTICLE TYPE

## Efficacious redox-responsive gene delivery in serum by ferrocenylated monomeric and dimeric cationic cholesterol

Gururaja Vulugundam,<sup>‡,a</sup> Krishan Kumar,<sup>‡,a</sup> Paturu Kondaiah<sup>b</sup> and Santanu Bhattacharya<sup>\*a</sup>

Received (in XXX, XXX) Xth XXXXXXXXX 20XX, Accepted Xth XXXXXXXXX 20XX

DOI: 10.1039/b000000x

Herein, we present the design and synthesis of new redox-active monomeric and dimeric (gemini) cationic lipids based on ferrocenylated cholesterol derivatives for gene delivery. The cationic cholesterol

are shown to be transfection efficient after being formulated with neutral helper lipid DOPE in the presence of serum (FBS). Redox activity of the resulting co-liposomes and their lipoplexes could be regulated using alkanyl ferrocene moiety attached with the ammonium headgroups of the cationic cholesterol. Atomic force microscopy (AFM), dynamic light scattering (DLS) and zeta potential measurements were performed to characterize the co-liposomal aggregates and their complexes with *p*DNA. The transfection efficiency of lipoplexes could be tuned by changing the oxidation state of the ferrocene moiety. Gene transfection capability was assayed in terms of green fluorescence protein (GFP) expression using *p*EGFP-C3 plasmid DNA in three cell lines of different origins, namely Caco-2, HEK293T and HeLa in the presence of serum. The vesicles possessing ferrocene in reduced state induced efficient transfection even better than a commercial reagent lipofectamine 2000 (Lipo 2000) as evidenced from flow cytometry and fluorescence microscopy. All the co-liposomes containing the oxidized ferrocene displayed diminished levels of gene expression. Gene transfection events from the oxidized co-liposomes were further potentiated by introducing ascorbic acid (AA) as a reducing agent during lipoplex incubation with cells, leading to the resumption of transfection activity. Assessment of transfection capability of both reduced and oxidized co-liposomes was also undertaken following cellular internalization of labelled *p*DNA using confocal microscopy and flow cytometry. Overall, we demonstrate here controlled gene transfection activities using redox-driven, transfection efficient cationic monomeric and dimeric cholesterol lipids. Such systems could be used in gene delivery applications where transfection is needed to be performed spatially or temporally.

### Introduction

Recently, there has been a surge in research activity in the development of gene and drug delivery systems that are also responsive to external stimuli.<sup>1-3</sup> These systems undergo reversible physical or chemical changes in response to external or internal stimuli like pH,<sup>4-6</sup> heat,<sup>7</sup> light,<sup>5</sup> presence of reducing agents<sup>8</sup> and enzymes<sup>9,10</sup> etc. In case of biological cells, membrane fusion and disassembly in response to an imposed membrane potential is a common phenomenon. Thus, stimuli responsive systems find applications in controlled and selective release of the enveloped cargo (DNA/drug) at the target site whenever it is required.

Ferrocene (Fc) is one of the most commonly used redox-switchable moiety because of its chemical stability over a wide range of solution conditions and favorable working redox potentials.<sup>11,12</sup> The transformation of hydrophobic ferrocene [Fc(II)] to hydrophilic ferrocenium [Fc(III)] moiety has been utilized by many groups to control the aggregation properties of a number of synthetic molecular systems.<sup>13</sup> Gokel and coworkers reported for the first time vesicle formation from a steroidal

derivative of ferrocene. These acted as pro-amphiphiles, which formed vesicles upon oxidation to ferrocenium moiety as a polar headgroup.<sup>14,15</sup> The vesicles collapsed when Fc(III) was reduced to Fc(II). Abe's group reported spontaneous vesicle formation by a mixture of cationic ferrocenyl surfactant (FTMA) and an anionic surfactant (SDBS) which were reversibly converted into micelles upon oxidation of FTMA and reformed into vesicles on reduction.<sup>16</sup> These authors also demonstrated vesicle formation by ferrocene terminated dialkyl chain surfactant, bis-(11-ferrocenyl-(undecyl)) dimethylammonium bromide (BFDMA) which disintegrated into smaller aggregates and micelles after oxidation.<sup>17,18</sup> Abbott *et al.* studied the interaction of BFDMA with DNA and successfully demonstrated spatial and temporal control over lipoplex mediated DNA delivery.<sup>19-29</sup> These authors showed that the oxidation state of Fc which was present in the hydrophobic domain, played a key role in mediating high or low levels of gene transfection.<sup>19,20</sup> It was also shown that these transfection 'inactive' lipoplexes can be "turned on" by chemically activating them both before and after the introduction

of lipoplexes to the cells.<sup>21,22</sup> Apart from this, a recent study with covalently attached ferrocene to the phospholipid headgroup permitted an electrochemical modulation of the liposomal membrane permeability.<sup>30</sup>

5 Cholesterol being an important constituent in the animal cell membranes, it is implicated in various biological processes.<sup>31-33</sup> As a part of our continuing efforts to develop efficient cationic lipids with improved gene delivery efficacies, we earlier reported several cholesterol based monomeric and gemini cationic lipids and studied their aggregate formation and DNA delivery efficiency.<sup>34-41</sup> However till date no ferrocene based cholesterol derivative has been developed which can also induce gene transfection. Herein, we report the gene delivery efficacies of ferrocene containing cationic monomeric and dimeric lipids based on cholesterol backbone (Fig. 1). The redox-active ferrocene moiety is located at the polar headgroup region in the monomeric lipid series while it is a part of the spacer joining the polar headgroups in the case of gemini lipid series. The lipoplexes formed from these redox-active lipids formulated with a helper lipid 1, 2-dioleoyl-*sn*-glycero-3-phosphatidyl ethanolamine (DOPE) showed excellent transfection ability, significantly better than a commercial formulation, lipofectamine 2000 (Lipo 2000) in the presence of serum. Importantly, the transfection activity could be controlled via a change in the redox state of the ferrocene moiety. The oxidation of ferrocene in liposomal formulations led to a decrease in the transfection capability of the resulting lipoplexes. The transfection activity could be resumed after exposing the oxidized lipoplexes to ascorbic acid (AA) in the cell culture medium. All the co-liposomes (Reduced and oxidized) and their transfection optimized lipoplexes were characterized using zeta, DLS and AFM measurements. Such transfection efficient systems with distinct activity under the influence of redox phenomenon could be very useful where cellular gene expression needs to be achieved in spatially or temporally controlled manner.

## Experimental Details

### Materials

All reagents and solvents used in the present study were of the highest grade commercially available and all solvents were used purified, dried, or freshly distilled, as required. Starting materials, such as ferrocene, 6-bromohexanoic acid, 11-bromoundecanoic acid, anhydrous aluminium chloride and sodium borohydride were purchased from Sigma-Aldrich. 1,2-Dioleoyl-*sn*-glycero-3-phosphatidyl ethanolamine (DOPE) was purchased from Avanti Polar Lipids. Column chromatography was performed using a 60-120 mesh silica gel. NMR spectra were recorded using a Bruker spectrometer (400 MHz for <sup>1</sup>H NMR and 100 MHz for <sup>13</sup>C NMR). The chemical shifts ( $\delta$ ) are reported in ppm downfield from the internal standard: TMS, for <sup>1</sup>H-NMR and <sup>13</sup>C-NMR. Mass spectra were recorded on a MicroMass ESI-TOF spectrometer. All the compounds were adjudged pure by <sup>1</sup>H NMR, <sup>13</sup>C NMR, mass spectroscopy (ESI-MS) and elemental analysis.

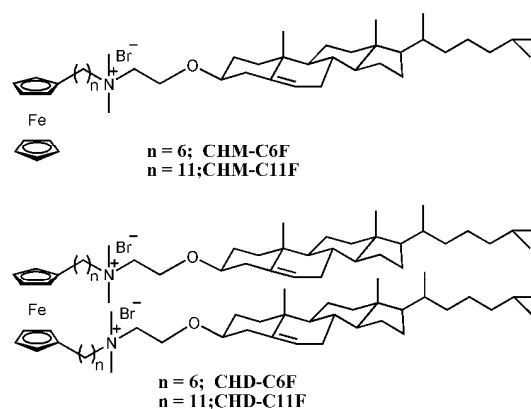


**Fig. 1** Molecular structures of redox-active ferrocene containing cationic monomeric (CHM-C6F and CHM-C11F) and gemini (CHD-C6F and CHD-C11F) cholesterol lipids.

### Synthesis

70 All the intermediates (1-8) and the final lipids (CHM-C6F, CHM-C11F, CHD-C6F and CHD-C11F) were prepared as described in the Supplementary Information (ESI†).

### Preparation of reduced and oxidized co-liposomes

Mixed liposomes of each cationic lipid with DOPE in the desired molar ratio were prepared by dissolving in chloroform in a wheaton glass vial. Organic solvent was evaporated by passing N<sub>2</sub> gas to form a thin film along the walls of the tube which was dried completely under vacuum for 6 h. Each lipid was then hydrated in presence of 1 mM aqueous Li<sub>2</sub>SO<sub>4</sub> solution (pH 6) which was filtered through 0.1  $\mu$ m cut-off Millex titration cartridges to remove any extraneous particles. The electrolyte was required for the electrolytic oxidation of the ferrocenylated liposomes. The final concentration of each cationic lipid was maintained at 1 mM which was left for hydration for 12 h at 4 °C and repeatedly freeze-thawed (ice-cold water to 70 °C) with intermittent vortexing to ensure optimal hydration. Sonication of these suspensions for 15 min in a bath sonicator at 70 °C afforded liposomes which were used for all the studies. Oxidized co-liposomes were prepared by electrochemical oxidation of the 1 mM suspension of reduced cationic lipid/DOPE as described earlier.<sup>29</sup> The cationic lipid suspensions were heated up to 70 °C and electrochemical oxidation was accomplished using a CHI 660A electrochemical analyzer (CH instruments, TX, USA) with a conventional three electrode assembly. Platinum mesh (4.0 cm<sup>2</sup>) was used as the working and auxiliary electrodes and saturated calomel electrode as the reference electrode. A constant potential of 600 mV was applied between the working electrode and a reference electrode along with continuous purging of N<sub>2</sub> gas. The progress of oxidation was followed by monitoring current passed at the working electrode and by UV/visible spectrophotometry. The UV-Vis spectra of the redox-active lipid suspensions before and after oxidation are presented in Fig. S1, ESI†. The absorption peak corresponding to ferrocene [Fc(II)] (430 nm) gets suppressed after oxidation and a new peak at 645 nm characteristic of ferrocenium moiety [Fc(III)] appeared. The oxidized co-liposomes appeared to be quite stable where the characteristic peak of ferrocenium was evident even after 96 h of oxidation (Fig. S1, ESI†).

### Dynamic Light Scattering (DLS) and Zeta Potential Measurements

The average particle sizes and the zeta potentials of the copliposomes were determined using the Zetasizer nano (Malvern, Worcestershire, UK) instrument which employed an incident laser beam of 633 nm wavelength. Mean diameters reported were obtained from Gaussian analysis of the intensity-weighted particle size distributions. The lipid concentrations for size and zeta potential measurements were maintained at 0.1 mM. Lipoplexes of the reduced or oxidized cationic lipid formulations at various lipid/*p*DNA molar ratios were prepared by mixing *p*DNA and a given amount of the cationic lipid formulation such that the final concentration of *p*DNA is 4 µg/mL. The DLS and zeta potential measurements were performed after an incubation of 30 min.

### Atomic Force Microscopy

AFM images were recorded on an atomic force microscope (AFM, JPK NanoWizard) by tapping mode in air. The aqueous suspensions were prepared as described above and deposited onto freshly cleaved mica. Immobilization was achieved using electrostatic forces between the opposed charges of mica and polymeric suspensions. The sample was carefully dried overnight in vacuum before each measurement. Lipoplexes were prepared as described above for the DLS measurements.

### Cell culture

Three different cell lines namely Caco-2, HEK293T and HeLa were cultured in cell culture media, DMEM (Dulbecco's modified Eagle's medium) containing 10% fetal bovine serum (FBS). Cell culture media also contained pen strep (100 units/ml penicillin and 100 µg/ml streptomycin) as an antibiotic. Cells were maintained in incubator (37 °C) at relative humidity > 95% with a CO<sub>2</sub> level of 5%. All the cell lines were passaged using 0.5 % trypsin-EDTA at proper confluency levels.

### Transfection Biology (EGFP Expression)

We used pEGFP-C3 plasmid DNA to check the gene transfection levels mediated by redox responsive cationic monomeric and gemini lipids. In a typical gene transfection experiment, first 24 well cell culture plates were seeded at the density of 40,000 cells/well and allowed to grow for 24 h. Lipoplexes were prepared using 0.8 µg of pEGFP-C3 plasmid DNA and different co-liposomal formulations at various molar ratios (cationic lipid/*p*DNA). Cells were treated with lipoplexes for 6 h in 10% serum (FBS) containing cell culture medium. The oxidized lipoplexes were incubated in cell culture media with and without ascorbic acid (10 molar equivalents of cationic lipid). After lipoplex treatment, cells were incubated for another 42 h. At the end, cells were washed twice properly with DPBS and detached by trypsinization using 0.5 % trypsin-EDTA. Cells were pooled in 5% FBS containing DPBS and taken for analysis using FACS Calibur flow cytometer (Becton-Dickinson). Flow cytometry data analysis was performed using WinMDI 2.9 program. Gene transfection capabilities of different liposomal formulations were expressed in terms of % GFP positive cells and Geometric Mean Fluorescence Intensity (MFI). The visual expression of GFP was undertaken with the help of fluorescence microscopy (Olympus

IX-81).

### In Vitro Cytotoxicity

An MTT [3-(4,5-dimethylthiazole-2-yl)-2,5-diphenyltetrazolium bromide] assay was used to evaluate the viabilities of cells treated with different lipoplexes following gene transfection experiment conditions. In a typical experiment, cells were treated with lipoplexes after 24 h post plating of cells. Lipoplexes were removed after 6 h and fresh 10% serum containing media (200 µL) was added to wells. After 38 h, MTT (20 µL, 5mg/ml in DPBS) was added to each well for 4 h. The assay was terminated by removing entire medium from wells, followed by addition of DMSO (200 µL) and reading absorbance at 570 nm on a microplate reader. Lipoplex treatment in each experiment was performed in triplicates and the results expressed here are based on at least three such independent experiments.

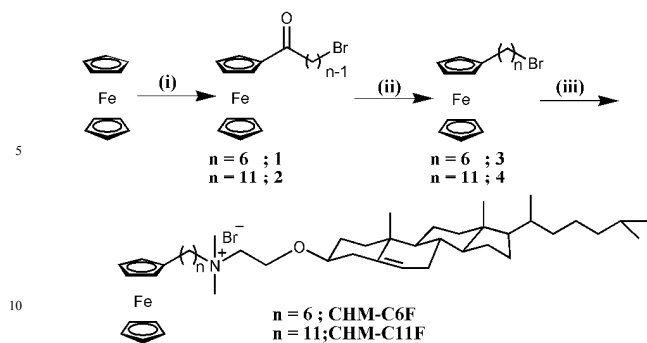
### Confocal Microscopy

Intracellular delivery of fluorescein labelled *p*DNA was followed using a confocal microscope. For microscopic analysis cells were first plated on glass cover slips in 12 well cell culture plates. Transfection experiments were performed using 1µg of labelled *p*DNA as discussed above. The molar ratios of maximum transfection efficiency for different formulations were taken into account for transfection experiment. The cells were washed twice properly with DPBS 48 h post transfection and fixed using 4% paraformaldehyde solution for 10 min. Again, after a proper wash with DPBS, cell nuclei staining was performed using DAPI (300 nM). Cells were again washed to remove excess of dye and the cover slips were mounted on glass slides over antifade reagent. Thus prepared samples were viewed under confocal laser scanning microscope (LSM meta, Zeiss).

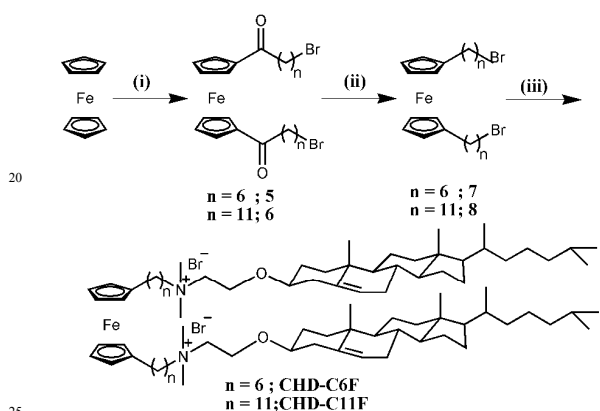
### Results and discussion

Earlier work from this laboratory showed a significant improvement in the transfection efficiency of cationic cholesterol based cytofectins when the cationic headgroup is linked to the steroid backbone via an ether type linkage as compared to its ester or urethane counterparts.<sup>42,43</sup> Subsequent studies showed that cholesterol-based gemini lipids based on ether linkage with varying length of the spacer between the ammonium headgroups formed stable formulations which turned out to be also superior transfecting agents.<sup>35,36</sup> In the present work, we describe the effect of introducing a redox-active ferrocene moiety on the gene delivery capability of two series of redox-active cholesterol based cationic lipids. For the monomeric lipids (CHM-C6F and CHM-C11F), the redox-responsive ferrocene moiety was attached on to the cationic headgroup via either six carbon or eleven carbon spacer. In the case of the gemini lipids (CHD-C6F and CHD-C11F), the two cationic cholesterol units were connected via six and eleven carbon spacer on either side of the cyclopentadienyl rings of ferrocene. Here, the ferrocene moiety becomes a part of the polymethylene spacer which joins the two cationic headgroups. The synthesis of these cationic lipids as outlined in scheme 1 and scheme 2 was accomplished as briefly described below.

110



**Scheme 1 Reaction conditions.** (i)  $\omega$ -Bromoalkanoyl chloride, anhyd.  $\text{AlCl}_3$ ,  $\text{CH}_2\text{Cl}_2$ , RT, 12 h, 55-60%; (ii)  $\text{NaBH}_4/\text{AlCl}_3$ , THF, RT, 4h, 85-90%; (iii) Chol- $\text{OCH}_2\text{CH}_2\text{NMe}_2$ , MeOH-EtOAc (1:1), screw-top pressure tube, 70 °C, 40-50%.



**Scheme 2 Reaction conditions.** (i)  $\omega$ -Bromoalkanoyl chloride, anhyd.  $\text{AlCl}_3$ ,  $\text{CH}_2\text{Cl}_2$ , RT, 12 h, 45-55%; (ii)  $\text{NaBH}_4/\text{AlCl}_3$ , THF, RT, 4h, 75-80%; (iii) Chol- $\text{OCH}_2\text{CH}_2\text{NMe}_2$ , MeOH-EtOAc (1:1), screw-top pressure tube, 70 °C, 40-50%.

### 30 Chemistry

Briefly,  $\omega$ -bromo aliphatic-1-monoacylferrocenes (**1**, **2**) and  $\omega$ -bromo aliphatic-1,1'-diacylferrocenes (**5**, **6**) were synthesized by acylation of ferrocene using appropriate  $\omega$ -bromoalkanoyl chloride in the presence of anhydrous  $\text{AlCl}_3$  in dry  $\text{CHCl}_3$ . This was followed by the complete reduction of the ketone group by  $\text{NaBH}_4/\text{AlCl}_3$  in dry THF to produce 1-( $\omega$ -bromoalkyl) ferrocenes (**3**, **4**) and 1,1'-bis( $\omega$ -bromoalkyl) ferrocenes (**7**, **8**) respectively in 85-90 % and 75-80 % yield. Monomeric lipids (CHM-C6F and CHM-C11F) and gemini lipids (CHD-C6F and CHD-C11F) were obtained by refluxing the key precursor cholest-5-en-3 $\beta$ -oxyethan-*N,N*-dimethyl amine (Chol  $\text{OCH}_2\text{CH}_2\text{NMe}_2$ ) (0.2 mmol) with either **3** or **4** (0.22 mmol) and **7** or **8** (0.07 mmol) respectively in dry MeOH-EtOAc (4 mL, v/v : 1/1) over a period of 4-6 days in a screw-top pressure tube, until TLC indicated the completion of each reaction. After that, the reaction mixture was cooled and the solvent was evaporated to furnish a crude solid which was purified by column chromatography over neutral alumina using  $\text{CHCl}_3$  to  $\text{CHCl}_3$ -MeOH. The isolated yields of the pure lipids ranged from 40-50 %. The purities of these lipids were ascertained from TLC; the  $R_f$  ranged from 0.2 to 0.3 in 20:1 and 10:1  $\text{CHCl}_3/\text{MeOH}$  for the monomeric and gemini lipids, respectively. Each new lipid was fully characterized by  $^1\text{H-NMR}$ ,

$^{13}\text{C-NMR}$ , mass spectrometry and elemental analysis (ESI $^\dagger$ ).

### 55 Physicochemical Characterizations of co-liposomes

The co-liposomes (DOPE/cationic lipid) considered for physicochemical characterizations were those which showed maximum gene transfection capabilities (DOPE/CHM-C6F; 2.5:1, DOPE/CHM-C11F; 1.5:1, DOPE/CHD-C6F; 4:1 and DOPE/CHD-C11F; 3:1) as discussed in Gene Transfection Biology section.

### Atomic Force Microscopy (AFM)

We examined the shape and size distribution of the co-liposomal formulations containing each of the cationic ferrocenyl lipids along with DOPE at the optimized ratio (from gene transfection) by atomic force microscopy. Although the lipid suspensions from both, the reduced and oxidized lipids, formed nearly spherical vesicles they differed in their size. As shown in Fig. 2, we observed that the vesicles dilated upon oxidation. The co-liposomal formulations containing CHM-C6F in its reduced state formed vesicles of sizes 70-100 nm which upon oxidation increased to 120-150 nm. Similar trend was observed in the case of the dimeric redox lipid, CHD-C6F which increased in sizes from 120-150 nm to 160-200 nm after oxidation of ferrocene in co-liposomes. It may be noted that the net charges of these redox-active cationic lipids change upon oxidation. In the case of monomeric lipids, complete oxidation of ferrocene moiety of CHM-C6F and CHM-C11F to ferrocenium leads to a change in overall molecular charge from +1 to +2. On the other hand, for gemini lipids CHD-C6F and CHD-C11F, the net charge changes from +2 (reduced) to +3 (oxidized) upon complete oxidation. Thus it is likely that due to the increased electrostatic repulsions among the positively charged ferrocenium moieties along with that of the cationic ammonium headgroups, we observed larger liposomes.<sup>44</sup>

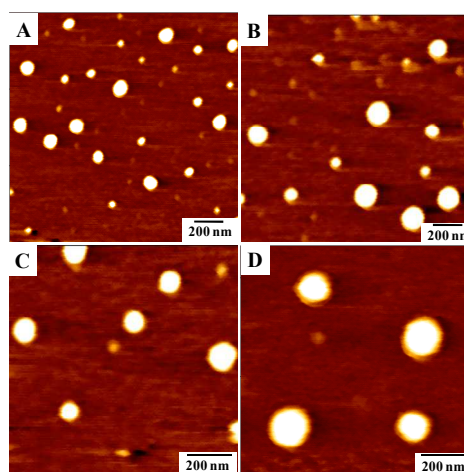


**Fig. 2** Representative atomic force micrographs of the co-liposomes of cationic ferrocenyl cholesterol and DOPE at the transfection optimized ratio. (A) CHM-C6F (Red.), (B) CHM-C6F (Ox.), (C) CHD-C6F (Red.) and (D) CHD-C6F (Ox.).

### Dynamic Light Scattering (DLS) and Zeta Potential measurements

The average hydrodynamic diameters and zeta potential of each redox lipid/DOPE mixed aggregates (transfection optimized) in

their unoxidized and oxidized state are shown in Table 1. When the ferrocene moiety is present in the native unoxidized state, monomeric lipid/DOPE (1:2.5, CHM-C6F and 1:1.5, CHM-C11F) suspensions formed aggregates of the size 130-150 nm while the gemini lipid/DOPE (1:4, CHD-C6F and 1:3, CHD-C11F) suspensions formed slightly larger aggregates of size 170-200 nm. In the case of the oxidized lipid/DOPE suspensions, the size of the resultant aggregates was found to be larger than that of their counterparts prior to oxidation. This could be due to the formation of ferrocenium species upon oxidation which probably introduced greater inter-lipidic repulsion in their vesicular aggregates. It may be noteworthy that the sizes of various ferrocenyl lipid/DOPE co-aggregates as obtained from the DLS studies were comparable to those obtained from the AFM measurements.

The mixed lipid suspensions were further characterized by zeta potential measurements which allowed the determination of the effective charge of the exposed surface of the lipid co-aggregates in aqueous media. As we moved from the monomeric to the gemini series, we observed an increase in the zeta potential of the liposomes from +30 mV to +43 mV. This may be due to the presence of two cationic ammonium headgroups present in the gemini lipids. All the oxidized lipid/DOPE formulations displayed much higher zeta potential values than their reduced counterparts. This could be ascribed to an increase in the global charge density of all the redox-active lipids upon oxidation of the ferrocene moiety.

**Table 1** Average Hydrodynamic Diameters and Zeta potentials of the redox-active cationic cholesterol/DOPE aggregates.<sup>a</sup>

Mixed Liposomes	Avg. hydrodynamic diameter (nm)		PDI		Zeta potential (mV)	
	Red.	Ox.	Red.	Ox.	Red.	Ox.
DOPE/CHM-C6F	130 ± 5	180 ± 25	0.14	0.22	31 ± 0.5	38 ± 2
DOPE/CHM-11F	145 ± 10	200 ± 20	0.11	0.25	30 ± 1	39 ± 2.5
DOPE/CHD-C6F	170 ± 10	225 ± 30	0.09	0.24	43 ± 1.7	51 ± 2
DOPE/CHD-C11F	195 ± 20	260 ± 30	0.16	0.28	41 ± 2	53 ± 3

<sup>a</sup> Hydrodynamic diameters and zeta potentials of co-liposomes of each redox-active cationic cholesterol/DOPE prepared in Li<sub>2</sub>SO<sub>4</sub> at the transfection optimized molar ratios. DOPE:CHM-C6F (2.5:1), DOPE:CHM-C11F (1.5:1), DOPE:CHD-C6F (4:1) and DOPE:CHD-C11F (3:1). The measurements were performed at a final cationic lipid concentration of 0.1 mM. Each value is a mean ± S.D of five independent measurements. PDI: Polydispersity index.

Additionally, we performed the DLS and zeta potential measurements of all co-liposomes prepared in 10 mM HEPES buffer (pH = 7.4) and compared with the liposomes prepared in Li<sub>2</sub>SO<sub>4</sub> as shown in Table S1, ESI†. We did not observe any significant change in the sizes of the co-liposomes prepared in Li<sub>2</sub>SO<sub>4</sub> and HEPES buffer (pH = 7.4). However, we found a slight decrease in zeta potential values in case of co-liposomes prepared in HEPES buffer than those in Li<sub>2</sub>SO<sub>4</sub>.

#### X-ray diffraction (XRD) Analysis

In order to provide a plausible illustration of the lipid molecular arrangement in the bilayer, we performed X-ray diffraction

(XRD) experiments for self-supported cast films of the co-liposomes (Fig. S2, ESI†). The XRD analysis revealed a series of higher order reflections in their diffraction pattern that are characteristic of lamellar phases. The bilayer widths calculated from the first order diffraction peak using Bragg's equation ( $n\lambda = 2d \sin \theta$ ) for the co-liposomes of CHM-C6F and CHD-C6F were found to be 37.8 Å and 45.1 Å respectively. Based on the energy optimized structure, the theoretical bilayer width of each lipid which is twice the distance from 'head' nitrogen atom to 'tail' terminal carbon is known to be 42 Å.<sup>34</sup> The lower value of theoretical bilayer widths for monomeric lipid than that of experimentally obtained values suggests that the co-liposomes of the monomeric lipids could adopt an interdigitated bilayer arrangement with the ferrocene alkyl chain being looped into the bilayer owing to its hydrophobic nature. Similarly, the experimentally obtained bilayer widths for gemini lipids were approximately similar with the theoretical value which suggested that the co-liposomes of gemini lipid could assume a regular bilayer like structure where the hydrophobic spacer consisting of 1,1'-dialkyl ferrocene could also loop into the bilayer to avoid its unfavourable contact with water (Fig. S3, ESI†).

#### Gene Transfection Biology

To assess the gene transfection capability of ferrocenylated cationic monomeric and dimeric cholesterols, we conducted transfection experiments in human epithelial colorectal adenocarcinoma (Caco-2) cells, human embryonic kidney (HEK) 293T cells and human epithelial cervical carcinoma (HeLa) cells. Transfection experiments were carried out using 0.8 µg of pEGFP-C3 plasmid DNA (pDNA) in 10% serum (FBS) containing cell culture medium (DMEM). Flow assisted cell sorting (FACS) was undertaken to quantify the transfection levels both in terms of the number of the cells showing the GFP expression in the transfected population (% GFP positive cells) and the level of GFP expression (Mean Fluorescence Intensity *i.e.* MFI). In order to prepare the co-liposomal formulations, each of the cationic lipids was admixed with neutral helper phospholipid, DOPE at different molar ratios (DOPE/lipid; 0.5:1 to 3:1 for the monocationic lipids and 1:1 to 6:1 for the dimeric lipids) which afforded stable co-liposomes.

Gene transfection experiments were first performed in Caco-2 cells in the presence of 10% serum (FBS) to optimize the best proportion of DOPE in liposomal formulations leading to maximum transfection efficiencies. Formulations with varying DOPE/cationic cholesterol were used to transfect pDNA at a fixed molar ratio (cationic lipid/pDNA) of 1:1 and 0.5:1 for monomeric and gemini cholesterols respectively. Monocationic cholesterols CHM-C6F and CHM-C11F showed maximum transfection efficiency at relatively lower DOPE ratios of 2.5:1 and 1.5:1 respectively than the gemini lipids CHD-C6F and CHD-C11F which showed maximum transfection efficiency at DOPE ratios 4:1 and 3:1 respectively (Fig. S4, ESI†).

All the DOPE optimized formulations of monomeric and gemini cholesterols as discussed above were used in subsequent gene transfection studies. We used different cationic cholesterol/pDNA ratios (molar ratios) to elicit maximum

transfection efficacies. The range of molar ratios used for the monomeric and gemini cholesterol were 0.5:1 to 2:1 and 0.25:1 to 1:1 respectively. We analyzed GFP expression for various controls, *i.e.*, cell alone, cells treated with only co-liposomes (at various concentrations used in different molar ratios) and cells treated with *p*DNA alone (0.8  $\mu$ g) which did not reveal any noticeable activity (Fig. S5, ESI<sup>†</sup>). Transfection data obtained from the flow cytometry for lipoplexes of various co-liposomes revealed that the cationic lipids CHM-C6F and CHD-C6F with C6 alkyl chain exhibited optimal GFP expression in Caco-2 cells that was significantly better than that of a commercial formulation, Lipofectamine 2000 (Lipo 2000). The transfection activity of the cationic lipid with C11 alkyl chain, CHM-C11F also appeared to be better than Lipo 2000 and CHD-C11F remained comparable to Lipo 2000 (Fig. 3). Among cationic monomeric lipids, CHM-C6F appeared to be relatively better gene transfectant than CHM-C11F. In case of gemini lipids, also the lipid with C6 alkyl chain showed better GFP expression than the ones with C11 alkyl chain.

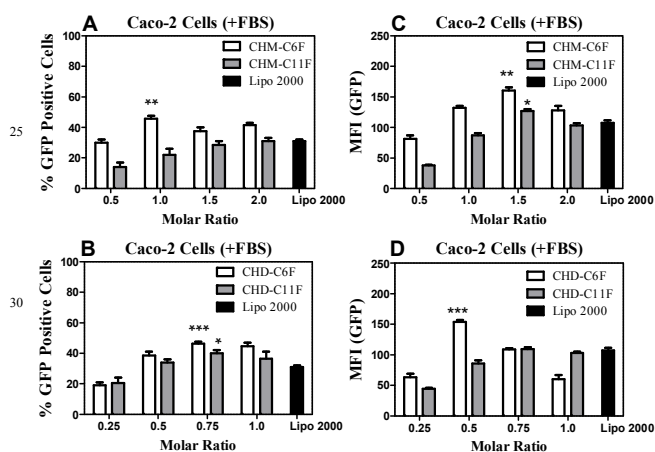


**Fig. 3** Optimization of maximum transfection activity of redox-active cationic monomeric (A and C) and gemini cholesterol (B and D) in Caco-2 cells. EGFP expression profile is represented as (A and B) % GFP positive cells and (C and D) mean fluorescence intensity (MFI). Transfection studies were performed using *p*DNA (*p*EGFP-C3, 0.8  $\mu$ g) in 10% FBS containing cell culture medium and GFP expression was analyzed 48 h post transfection. Transfection activities were analyzed for statistical significance in comparison with lipo 2000 (\* $P$  < 0.05, \*\* $P$  < 0.01 and \*\*\* $P$  < 0.001, Two-tailed Student's *t*-test).

Transfection experiments in HEK 293T cells also revealed the same order of transfection capability of cationic cholesterol as it was observed in Caco-2 cells. Cationic cholesterol with C6 alkyl chain (CHM-C6F and CHD-C6F) showed relatively better gene expression in comparison to that of Lipo 2000 (Fig. 4). However, the cationic lipid with C11 alkyl chain showed relatively lower expression of GFP.

Transfection studies were also performed in HeLa cells. Interestingly both the set of cationic cholesterol with C6 and C11 alkyl chain showed good expression of GFP which was also higher than the commercial formulation (Fig. 4). Cationic monomeric cholesterol showed relatively better transfection capability than their gemini (dimeric) counterparts. Among the gemini lipids, the one with C6 alkyl chain was slightly better than the one with C11 alkyl chain. GFP expression was also analyzed

using fluorescence microscopy where the level of GFP expression was in good agreement with the data obtained from flow cytometry in all the cell lines examined (Fig. 6).

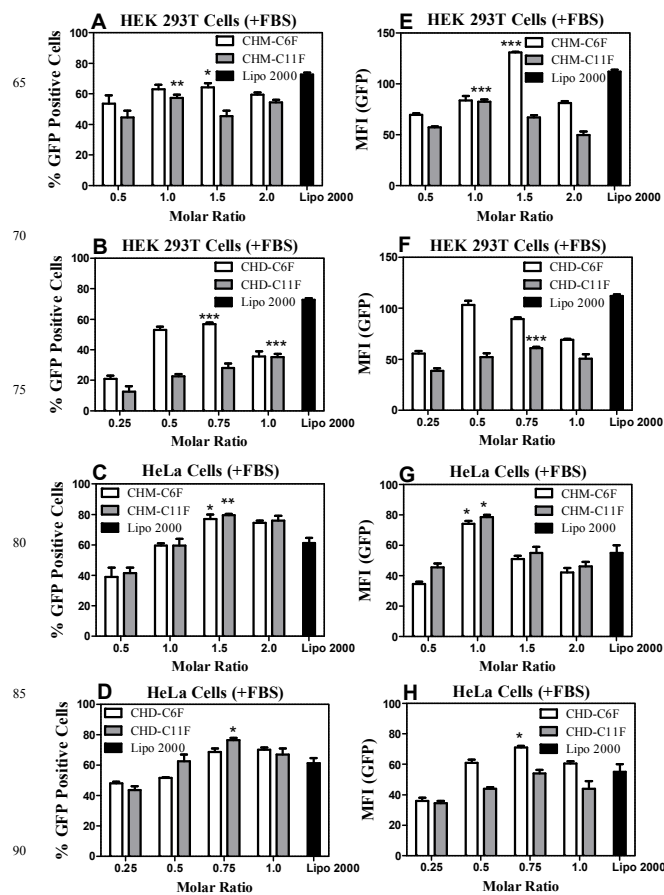


**Fig. 4** Optimization of transfection activity of the redox-active cationic monomeric (A, C, E and G) and gemini cholesterol (B, D, F and H) in HEK 293T and HeLa cells. GFP expression profile is represented as (A, B, C and D) % GFP positive cells and (E, F, G and H) mean fluorescence intensity (MFI). Transfection studies were performed using *p*DNA (*p*EGFP-C3, 0.8  $\mu$ g) in 10% FBS containing cell culture medium and GFP expression was analyzed 48 h post transfection. Transfection activities were analyzed for statistical significance in comparison with lipo 2000 (\* $P$  < 0.05, \*\* $P$  < 0.01 and \*\*\* $P$  < 0.001, Two-tailed Student's *t*-test).

### Oxidation state of ferrocene, a key determinant of the transfection efficiency

After the optimization of the maximum transfection activity mediated by cationic monomeric and gemini cholesterol which had ferrocene moiety in the unoxidized neutral state, we proceeded to check the transfection efficacies of these lipids after oxidation of the ferrocene. Each of the transfection experiment involved freshly prepared oxidized co-liposomes for lipoplex preparation. The lipoplexes derived from oxidized co-liposomes led to significantly reduced levels of gene transfection at all the molar ratios studied in each cell line. The oxidation state of ferrocene was found to have profound effect on gene transfection efficacies of both cationic monomeric and gemini cholesterol wherein GFP expression especially in terms of mean fluorescence

intensity (MFI) dropped down drastically. It should be noted that transfections with higher and lower MFI values reveal high and low GFP expression respectively.<sup>45</sup> This in turn reported that co-liposomes of the cationic cholesterol lost their transfection activity after oxidation of ferrocene (Fig. 5).

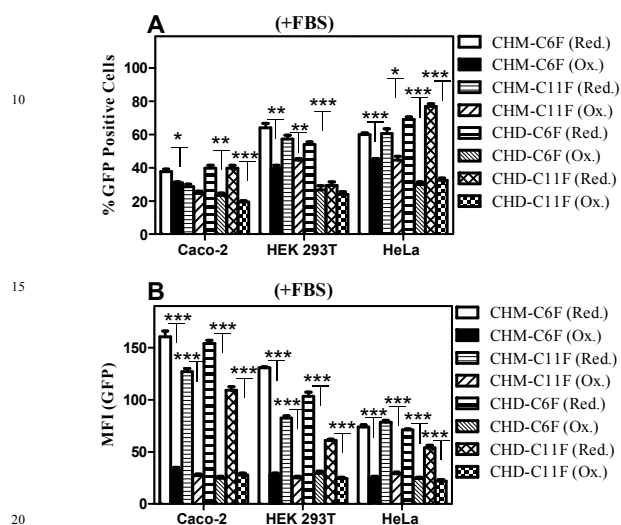


**Fig. 5** Effect of oxidation of ferrocene on the transfection activity of optimized lipoplexes (Red.) of monomeric and gemini cholesterol in Caco-2, HEK 293T and HeLa cell lines. Transfection efficacies are represented as % GFP positive cells (A) and mean fluorescence intensity (B). Transfections were performed using *pDNA* (pEGFP-C3, 0.8 $\mu$ g) in 10% FBS containing cell culture medium and GFP expression was analyzed 48 h post transfection. Transfection activities of oxidized co-liposomes were analyzed for statistical significance in comparison with reduced co-liposomes (\* $P$  < 0.05, \*\* $P$  < 0.01 and \*\*\* $P$  < 0.001, Two-tailed Student's *t*-test).

The differences in GFP expression in all the three cell lines were also analyzed using fluorescence microscopy where cells treated with lipoplexes containing cationic cholesterol with oxidized ferrocene showed significantly lower level of GFP expression when compared to the lipoplexes of reduced co-liposomes. Representative images of GFP expression for transfections mediated by reduced and oxidized CHM-C6F co-liposomes are shown below as a comparison. Transfection using Lipo 2000 following manufacturers protocol has also been shown as positive control (Fig. 6).

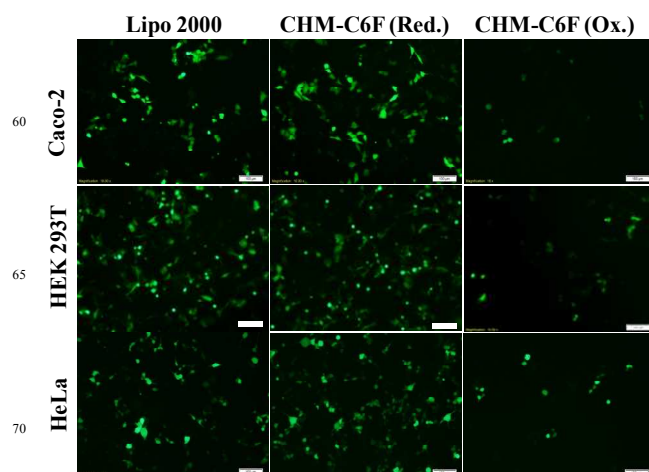


**Fig. 6** Representative fluorescence microscopic images for comparison of the GFP expression obtained from transfections mediated by CHM-C6F co-liposomes (Red. and Ox.) in all the three cell lines (Caco-2, HEK 293T and HeLa) while using Lipo 2000 as a positive control. Images were taken 48 h post transfection. Scale bar = 100  $\mu$ m.

We also looked at the gene expression levels in higher serum concentration where lipoplex incubation with cells was performed in 50% serum concentration. We chose CHM-C6F which showed significant levels of gene expression in all the three cell lines in the presence of 10% serum concentration. Higher serum concentration of course reduced the transfection efficiency of reduced co-liposomes slightly while transfections mediated by oxidized ferrocene based lipoplexes were still inactive (Fig. S6, ESI<sup>†</sup>). GFP expression analysis using fluorescence microscopy substantiated the flow cytometry data where oxidized co-liposome transfected cells showed significantly lower intensity of GFP expression (Fig. S7, ESI<sup>†</sup>). This observation was in accordance with previously reported literature on other ferrocene based carriers.<sup>19,20</sup>

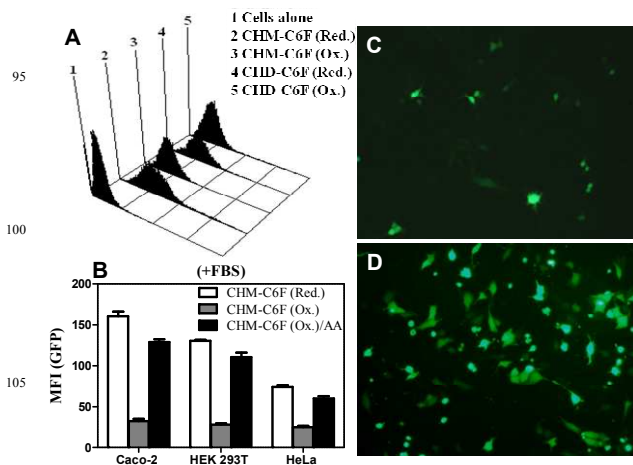
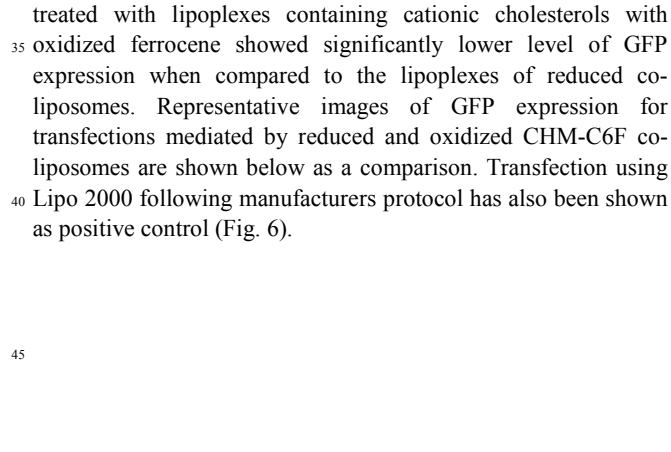


**Fig. 7** (A) Representative flow cytometry histograms for the cellular internalization of labelled *pDNA* after 6 h lipoplex treatment in HeLa cells in the presence of 10% serum containing medium. (B) GFP expression (MFI) profile derived from the treatment of lipoplexes of CHM-C6F (Red. and Ox.) and AA treated oxidized lipoplexes. Fluorescence microscopic images of HeLa cells depicting GFP expression in transfections mediated by AA treated CHM-C6F (Ox.) lipoplexes (D) in comparison with CHM-C6F (Ox.) lipoplexes (C).



Once the transfection levels were optimized for both reduced and oxidized ferrocenylated cholesterol containing lipoplexes, we made the study by asking whether the transfection activity of oxidized lipoplexes could be resumed by following the reduction of lipoplexes by ascorbic acid (AA) as reported elsewhere.<sup>22</sup> Interestingly, transfections performed by CHM-C6F (Ox.) in AA containing cell culture media could lead to gene expression levels comparable to that of CHM-C6F (Red.) and the phenomenon was quite reproducible in all the three cells lines studied (Fig. 7B). This was also confirmed by visual analysis made under fluorescence microscope where ostensibly significant difference in GFP expression was observed for CHM-C6F (Ox.) treatment and CHM-C6F (Ox.)/AA treatment (Fig. 7C and 7D). This could be attributed to the extracellular exposure of the oxidized lipoplexes to AA leading to activity resumption after reduction. Thus, the liposomal formulations shown here could be harnessed under the influence of redox response with trenchant control extracellularly. Such phenomenon could be quite useful for gene delivery applications where the gene expressions are likely to be considered spatially or temporally. This controlled activation of inactive lipoplexes could also help the delivery of DNA molecules to a specific cell population.

EGFP expression originated from the lipoplexes derived from the co-liposomal formulations containing the reduced and oxidized ferrocene was also followed at the level of intracellular delivery of labelled *p*DNA using flow cytometry and confocal microscopy experiments. HeLa cells were transfected with fluorescein labelled *p*DNA-lipoplexes derived from the reduced or oxidized CHM-C6F and CHD-C6F co-liposomes for an incubation period of 6h and analyzed under flow cytometer. It showed that greater *p*DNA fluorescence was observed in the cells transfected with lipoplexes of reduced co-liposomes than that of oxidized ones (Fig. 7A). A representative quantification for *p*DNA fluorescence positivity in CHM-C6F co-liposome (Red. and Ox.) transfected HeLa cells is also shown in Fig. S8 (ESI<sup>†</sup>) wherein the reduced and oxidized co-liposome transfected cells showed ~80% and ~30% *p*DNA fluorescence positivity respectively. To corroborate the observation we undertook confocal microscopy experiments. Interestingly, higher *p*DNA fluorescence was observed in the HeLa cells transfected with reduced CHM-C6F co-liposomes and as expected, lower number of cells was found to exhibit *p*DNA fluorescence after transfection with oxidized CHM-C6F co-liposomes as shown in Fig. 8A and 8B. Lipo 2000 served as a positive control in the experiment and the observed *p*DNA fluorescence appeared almost similar to reduced CHM-C6F as shown in Fig. 8C.

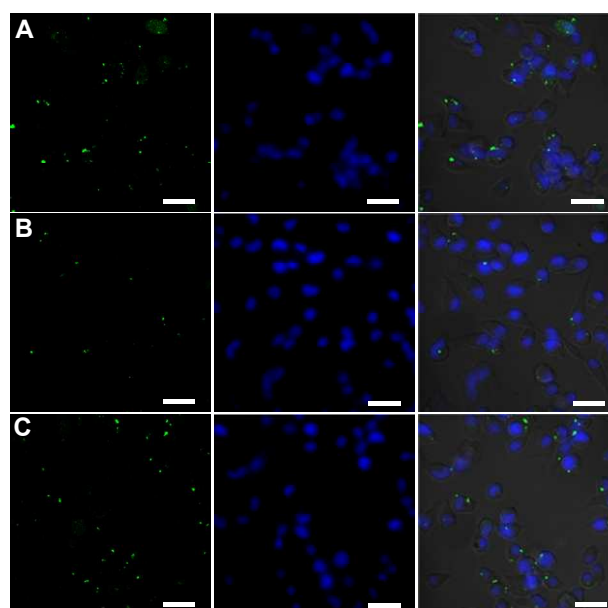


**Fig. 8** Confocal microscopy images of HeLa cells after 6 h of lipoplex treatment in the presence of serum. Lipoplex treatments consisted of CHM-C6F (Red.) (A), CHM-C6F (Ox.) (B) and Lipo 2000 as a positive control (C). Panels A, B and C represent (left to right) *p*DNA fluorescence, DAPI stained nuclei and overlay of previous two along with bright field images. Lipoplexes were prepared using 1  $\mu$ g of fluorescein labelled *p*DNA at molar ratios of maximum transfection and incubated for 30 min before adding to the cells. Scale bar = 20  $\mu$ m.

#### Characterization of the lipoplexes

Physical properties like the aggregate size and zeta potential are crucial parameters which influence the transport of DNA across the cell membranes.<sup>46, 47</sup> We performed dynamic light scattering measurements to characterize the lipoplexes prepared from *p*DNA and the co-liposomes of redox-active lipids. Fig. 9A shows the hydrodynamic size of lipoplexes obtained from both, the reduced and oxidized forms of the cationic cholesterol/DOPE formulations at various cationic cholesterol/*p*DNA molar ratios. At lower ratios, CHM-C6F co-liposomes formed lipoplexes of ~250 nm size which increased to 500 nm at molar ratio of 1 and then decreased to much smaller size of ~180 nm. On the other hand, the gemini lipid CHM-C6D co-liposomes in the reduced state formed lipoplexes of relatively larger size (~350 nm) at lower ratios and formed smaller sized lipoplexes (~200 nm) from molar ratio of 1 to 5. The lipoplexes formulated using oxidized CHM-C6F and CHD-C6F co-liposomes were considerably larger than the lipoplexes formed using their reduced counterparts at all the molar ratios investigated. This might be another reason for the low transfection capability of the oxidized lipid formulations.

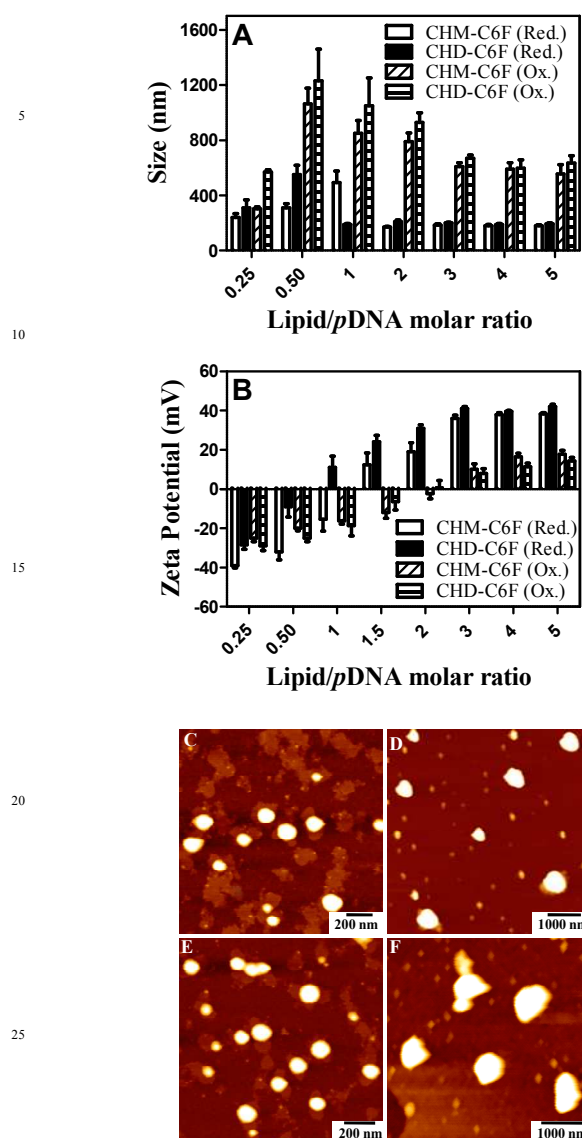


**Fig. 9** Hydrodynamic diameters (A) and zeta potentials (B) of lipoplexes formed using solutions of *p*DNA and co-liposomes of redox-active lipids at various lipid:*p*DNA molar ratios. Atomic force microscopic images of optimized lipoplexes of (C) CHM-C6F (Red.), (D) CHM-C6F (Ox.), (E) CHD-C6F (Red.) and (F) CHD-C6F (Ox.).

Fig. 9B illustrates the zeta potentials of the lipoplexes formed using reduced and oxidized lipids and *p*DNA at various molar ratios. Lipoplexes formed using the reduced forms of both, CHM-C6F and CHD-C6F co-liposomes showed a transition from negative to positive zeta potentials with increasing molar ratios with the change in sign occurring at molar ratio of 1.5 and 1 respectively. The oxidized forms of the lipid formulations under consideration also showed negative zeta potentials at lower ratios but showed much less positive values even at higher molar ratios.

We also measured zeta potentials and size of the representative oxidized lipoplexes (lipid/*p*DNA; molar ratio, 2) of CHM-C6F treated with ascorbic acid (AA). It revealed an evident increase in zeta potential values of oxidized lipoplexes after AA treatment (from  $-3.5 \pm 3$  mV to  $16 \pm 5$  mV) which was comparable to that of lipoplexes of reduced co-liposomes ( $19 \pm 6$  mV) (Fig. S9B,

ESI†). It was also observed that there was a significant decrease in the size of oxidized lipoplexes after AA treatment (from  $\sim 900$  nm to  $\sim 200$  nm) (Fig. S9A, ESI†). This could have possibly led to the resumption in transfection activity of oxidized lipoplexes upon treatment with AA.

The morphology of redox-active cationic lipids/*p*DNA were further investigated by atomic force microscopy, and all the lipoplexes were prepared at the molar ratio which showed optimum transfection efficiency. Lipoplexes formed from the cationic cholesterols in their reduced state were observed as near-spherical shaped aggregates with an average size of 100-200 nm (Fig. 9C and 9E). However, the lipoplexes formed from their oxidized counterparts exhibited larger particle sizes around 500-900 nm (Fig. 9D and 9F). This indicates that the particle size of the lipoplexes could be greatly influenced by the oxidation state of the redox-active cationic cholesterols. The plausible reason for the relatively larger size of the lipoplexes derived from oxidized co-liposomes could be their inability to effectively condense the *p*DNA into compact aggregates. This also resulted in lower zeta potential values due to the presence of loosely bound *p*DNA on the outer surfaces of these lipoplexes of oxidized co-liposomes. This might have led to poor transfection efficiency of oxidized co-liposomes. It may also be noticed that the lipoplex sizes observed by AFM are somewhat smaller than that observed from the DLS measurements. This variation in AFM and DLS results could be due to the shrinkage of the particles induced during the partial drying process for the AFM sample preparation, whereas, DLS data provide the sizes of 'intact' hydrated particles.<sup>48</sup> Interestingly when ferrocenes are located in the polar headgroup region, in the cationic cholesterols under current investigation, we observed higher zeta potential and smaller size for the lipoplexes formed from the cationic cholesterols in their reduced state. This might have led to better internalization by the cells which promoted high levels of transgene expression by the lipids with the ferrocene in its reduced state. This result is similar to an earlier report where the ferrocenes were at the end of the hydrophobic tails.<sup>29</sup>

#### 85 Cell Viability Assay

All transfection efficient formulations were screened for their toxicity using MTT assay towards all the cell lines used in the study following actual transfection experiment conditions. As a whole there was no obvious toxicity observed from the lipoplexes of all the cationic cholesterols except the monomeric lipid with C6 alkyl chain, CHM-C6F which appeared to give relatively lower cell viabilities. This trend was consistent among all the cell lines except that the monomeric lipid with C11 alkyl chain, CHM-C11F appeared to be slightly more toxic than CHM-C6F only in HeLa cells. All the formulations showed better cell viabilities when compared to commercial formulation, Lipo 2000 in all three cell lines. We observed that cationic gemini cholesterols appeared relatively less cytotoxic in comparison with the cationic monomeric cholesterols. Cell viability experiments revealed that transfection with lipoplexes containing lipids with oxidized ferrocene led to improved cell viabilities than the lipids with unoxidized ferrocene. Representative quantitation of cell viabilities is shown in Fig. 10 for all efficient formulations in three cell lines 48 h post transfection.

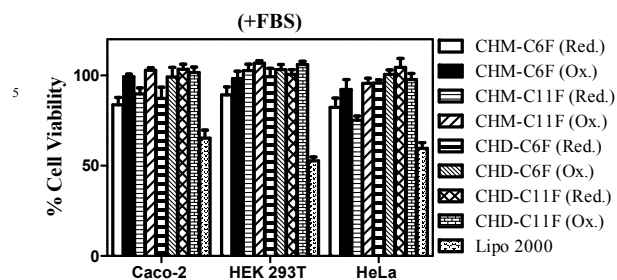


**Fig. 10** Cytotoxicity profile of all the transfection optimized lipoplexes of reduced and oxidized co-liposomes of monomeric and gemini cholesterol in Caco-2, HEK 293T and HeLa cells. Cell viability experiments (MTT assay) were performed following actual transfection conditions while using Lipo 2000 as a positive control. Experiments were conducted in triplicates and results presented here are based on such at least three independent experiments.

## Conclusions

We demonstrate here efficient *p*DNA delivery to three cell lines of different origins mediated by co-liposomes of cationic cholesterol lipids (monomeric and gemini) under the influence of redox control. The monomeric cholesterol possess ferrocene at head group region separated by alkanediyl spacers of different lengths (six and eleven methylene units). In the gemini cholesterol, ferrocene unit is flanked by alkanediyl chains on its both the cyclopentadienyl rings, forms the part of spacer segment which connects the cationic headgroups of the monomeric units. The oxidation state of the ferrocene moiety in the cationic cholesterol (that is, whether they are present in the reduced or oxidized state) is a critical determinant to mediate cell transfection. Co-liposomal formulations possessing ferrocenylated cholesterol in its natural unoxidized state are shown to produce high GFP levels even better than that of Lipofectamine 2000 in the presence of serum. On the other hand, oxidized ferrocenylated cholesterol exhibited significantly diminished levels of GFP expression. The transfection activities could easily be resumed after exposure of oxidized lipoplexes to ascorbic acid (AA). GFP expression observed under fluorescence microscopy was in good agreement with the flow cytometry (FACS) results. Transfection experiments conducted using fluorescein labelled *p*DNA showed higher lipoplex internalization for reduced co-liposomes than the oxidized ones. Lipoplexes derived from these liposomal formulations did not impart any acute toxicity in the range of optimized transfection concentration level. All the co-liposomal formulations and their lipoplexes were thoroughly characterized by means of DLS, zeta potential and AFM measurements. Overall, the transfection efficient redox-active cholesterol presented here could be useful for the on-demand/controlled and effective delivery of *p*DNA to cancer cells under the influence of redox sensitive behavior of ferrocene moiety.

## Notes and references

- <sup>a</sup>Department of Organic Chemistry, Indian Institute of Science, Bangalore, 560012, India. Fax: +91-80-23600529; Tel: +91-8022932664; E-mail: sb@orgchem.iisc.ernet.in
- <sup>b</sup>Department of Molecular Reproduction Development and Genetics, Indian Institute of Science, Bangalore, 560012, India. E-mail: paturu@mrdg.iisc.ernet.in
- ‡ These authors contributed equally to this work.
- † Electronic Supplementary Information (ESI) available: [Synthetic procedures and characterization details, DLS and zeta measurements of co-liposomes in HEPES buffer, UV-Vis spectra, XRD spectra of co-liposomes, Schematic illustration of lipid packing, Optimization of DOPE content in liposomal formulations and Transfection efficacies in 50% serum, FACS analysis of labelled *p*DNA internalization]. See DOI: 10.1039/b000000x/
- X. Guo and F. C. Szoka, *Acc. Chem. Res.*, 2003, **36**, 335.
  - P. Brown, C. P. Butts and J. Eastoe, *Soft Matter*, 2013, **9**, 2365.
  - M. S. Shim and Y. J. Kwon, *Adv. Drug Del. Rev.*, 2012, **64**, 1046.
  - V. Budker, V. Gurevich, J. E. Hagstrom, F. Bortzov and J. A. Wolff, *Nat. Biotechnol.*, 1996, **14**, 760.
  - O. V. Gerasimov, J. A. Boomer, M. M. Qualls and D. H. Thompson, *Adv. Drug Deliv. Rev.*, 1999, **38**, 317.
  - D. C. Drummond, M. Zignani and J. C. Leroux, *Prog. Lipid Res.*, 2000, **39**, 409.
  - M. B. Yatvin, J. N. Weinstein, W. H. Dennis and R. Blumenthal, *Science*, 1978, **202**, 1290.
  - Z. H. Huang, W. J. Li, J. A. MacKay and F. C. Szoka, *Mol. Ther.*, 2005, **11**, 409.
  - P. Meers, *Adv. Drug Deliv. Rev.*, 2001, **53**, 265.
  - C. Wang, Q. Chen, Z. Wang and X. Zhang, *Angew. Chem., Int. Ed.*, 2010, **49**, 8612.
  - K. Hoshino, K. Suga and T. Saji, *Chem. Lett.*, 1986, 979.
  - T. Saji, K. Hoshino and S. Aoyagui, *J. Am. Chem. Soc.*, 1985, **107**, 6865.
  - R. L. McCarley, *Annu. Rev. Anal. Chem.*, 2012, **5**, 391.
  - J. C. Medina, I. Gay, Z. Chen, L. Echegoyen and G. W. Gokel, *J. Am. Chem. Soc.*, 1991, **113**, 366.
  - K. Wang, S. Munoz, L. Zhang, R. Castro, A. E. Kaifer and G. W. Gokel, *J. Am. Chem. Soc.*, 1996, **118**, 6707.
  - H. Sakai, H. Imamura, Y. Kakizawa, Y. Kondo, N. Yoshino and M. Abe, *Colloids Surf. A: Physicochem. Eng. Aspects*, 2004, **232**, 221.
  - Y. Kakizawa, H. Sakai, K. Nishiyama and M. Abe, *Langmuir*, 1996, **12**, 921.
  - Y. Kakizawa, H. Sakai, A. Yamaguchi, Y. Kondo, N. Yoshino and M. Abe, *Langmuir*, 2001, **17**, 8044.
  - N. L. Abbott, C. M. Jewell, M. E. Hays, Y. Kondo and D. M. Lynn, *J. Am. Chem. Soc.*, 2005, **127**, 11576.
  - C. M. Jewell, M. E. Hays, Y. Kondo, N. L. Abbott and D. M. Lynn, *J. Controlled Release*, 2006, **112**, 129.
  - C. M. Jewell, M. E. Hays, Y. Kondo, N. L. Abbott and D. M. Lynn, *Bioconjugate Chem.*, 2008, **19**, 2120.
  - B. S. Aytar, J. P. E. Muller, S. Golan, S. Hata, H. Takahashi, Y. Kondo, Y. Talmon, N. L. Abbott and D. M. Lynn, *J. Controlled Release*, 2012, **157**, 249.
  - B. S. Aytar, J. P. E. Muller, Y. Kondo, Y. Talmon, N. L. Abbott and D. M. Lynn, *J. Am. Chem. Soc.*, 2013, **135**, 9111.
  - S. Golan, B. S. Aytar, J. P. E. Muller, Y. Kondo, D. M. Lynn, N. L. Abbott and Y. Talmon, *Langmuir*, 2011, **27**, 6615.
  - M. E. Hays, C. M. Jewell, Y. Kondo, D. M. Lynn and N. L. Abbott, *Biophys. J.*, 2007, **93**, 4414.
  - C. L. Pizzey, C. M. Jewell, M. E. Hays, D. M. Lynn, N. L. Abbott, Y. Kondo, S. Golan and Y. Talmon, *J. Phys. Chem. B*, 2008, **112**, 5849.
  - M. E. Hays, C. M. Jewell, D. M. Lynn and N. L. Abbott, *Langmuir*, 2007, **23**, 5609.
  - B. S. Aytar, J. P. E. Muller, S. Golan, Y. Kondo, Y. Talmon, N. L. Abbott and D. M. Lynn, *J. Colloid Interface Sci.*, 2012, **387**, 56.
  - J. P. E. Muller, B. S. Aytar, Y. Kondo, D. M. Lynn and N. L. Abbott, *Soft Matter*, 2012, **8**, 6608.

- 30 C. L. Debby, A. A. Arnold and J. Mauzeroll, *J. Am. Chem. Soc.*, 2010, **132**, 15120.
- 31 M. S. Brow and J. L. Goldstein, *Cell*, 1997, **89**, 331.
- 32 M. T. Bengoechea-Alonso and J. Ericsson, *Curr. Opin. Cell Biol.*,  
5 2007, **19**, 215.
- 33 K. Simons and D. Toomre, *Nat. Rev. Mol. Cell Biol.*, 2000, **1**, 31.
- 34 S. Bhattacharya and Y. K. Ghosh, *Langmuir*, 2001, **17**, 2067.
- 35 A. Bajaj, P. Kondaiah and S. Bhattacharya, *J. Med. Chem.*, 2007, **50**,  
2432.
- 10 36 A. Bajaj, P. Kondaiah and S. Bhattacharya, *Bioconjugate Chem.*, 2007,  
**18**, 1537.
- 37 S. Bhattacharya and J. Biswas, *Langmuir*, 2010, **26**, 4642.
- 38 A. Bajaj, P. Kondaiah and S. Bhattacharya, *J. Med. Chem.*, 2008, **51**,  
2533.
- 15 39 J. Biswas, S. K. Mishra, P. Kondaiah and S. Bhattacharya, *Org.*  
*Biomol. Chem.*, 2011, **9**, 4600.
- 40 S. K. Misra, S. Naz, P. Kondaiah and S. Bhattacharya, *Biomaterials*,  
2014, **35**, 1334.
- 41 S. K. Misra, J. Biswas, P. Kondaiah and S. Bhattacharya, *PLoS ONE*,  
20 2013, **8**, e68305.
- 42 Y. K. Ghosh, S. S. Visweswariah and S. Bhattacharya, *FEBS Lett.*,  
2000, **473**, 341.
- 43 Y. K. Ghosh, S. S. Visweswariah and S. Bhattacharya, *Bioconjugate*  
*Chem.*, 2002, **13**, 378.
- 25 44 Z. Wang, H. Mohwald and C. Gao, *Langmuir*, 2011, **27**, 1286.
- 45 P. Chabaud, M. Camplo, D. Payet, G. Serin, L. Molreau, P.  
Barthelemy and M. W. Grinstaff, *Bioconjugate Chem.*, 2006, **17**, 466.
- 46 B. Ma, S. Zhang, H. Jiang, B. Zhao and H. Lv, *J. Controlled Release*,  
2007, **123**, 184.
- 30 47 Z. U. Rehman, I. S. Zuhorn and D. Hoekstra, *J. Controlled*  
*Release*, 2013, **166**, 46.
- 48 C.M. Hoo, N. Starostin, P. West and M. L. Mecartney, *J. Nanopart.*  
*Res.*, 2008, **10**, 89.